



Regular paper

Associations between light-harvesting complexes and Photosystem II from *Marchantia polymorpha* L. determined by two- and three-dimensional electron microscopy

Roswitha Harrer

Max-Planck-Institut für Biophysik, Abteilung Strukturbiologie, Marie-Curie-Str. 13–15, D-60439 Frankfurt am Main, Germany; Present address: Völklinger Weg 21B, D-60529 Frankfurt am Main, Germany (e-mail: roswitha.harrer@freenet.de; fax: +49-69-6303-3002)

Received 10 October 2002; accepted in revised form 30 December 2002

Key words: electron microscopy, light-harvesting complexes, liverworts, *Marchantia polymorpha*, Photosystem II, random conical tilt, single-particle analysis, three-dimensional reconstruction

Abstract

Assemblies of Photosystem II and light-harvesting proteins were purified from the liverwort *Marchantia polymorpha* and investigated by two- and three-dimensional transmission electron microscopy of negatively stained specimens. By single-particle analysis, it was determined that about 25% of the particles are rectangular or slightly S-shaped with dimensions of 285 Å in length, 144 Å in width, 84 Å in height, while the membrane part is about 52 Å thick. This structure reveals the same architecture as that of a Photosystem II–light-harvesting assembly from seed plants. An overlay of the projection structure of the liverwort's complex with a projection structure deduced from stained trimeric LHC II crystals from pea confirmed the locations of trimeric LHC II within the liverwort's complex. Remarkably tight associations of LHC II and other chlorophyll *a/b* binding proteins with the PS II core complex are observed. More than 50% of the Photosystem II particles from the liverwort carry one or two additional masses. These extra masses are found to consist of an additional LHC II trimer and probably a chlorophyll *a/b* binding protein. For the first time, a three-dimensional structure of such a large assembly is defined.

Abbreviations: CAB – chlorophyll *a/b* binding; Chl – chlorophyll; CP – chlorophyll binding protein; DDM – β -dodecyl maltoside; EDTA – ethylene diamine tetraacetic acid; HEPES – 2,4-(2-hydroxyethyl)-1-piperazinyl ethane sulfonic acid; LHC – light-harvesting complex; MES – β -morpholinoethane sulfonic acid; PAGE – polyacrylamide gel electrophoresis; PS – Photosystem; SDS – sodium dodecyl sulfate

Introduction

Light-harvesting systems surround the photosynthetic reaction centers and serve as an inner and outer antenna. Two chlorophyll-binding proteins, CP43 and CP47, form the inner antenna of Photosystem (PS) II. Reaction center and inner antenna comprise the so-called core complex, which in green algae and land plants is further surrounded by an outer antenna composed of nuclear encoded chlorophyll *a* and *b* binding proteins (CAB proteins). CAB proteins function as

accessory antenna proteins and, due to their content of carotenoids, have an equally important role in protection against a damaging excess of light (Bassi et al. 1993; Jansson 1994; Paulson 1995; Yamamoto and Bassi 1996; Jansson 1999). Among the CAB proteins, the most abundant type is a trimeric pigment-protein complex (LHC II) composed of the *lhcb1*, 2, and 3 gene products. Its structure has been determined to 3.4 Å (Kühlbrandt et al. 1994). The structurally related but monomeric CAB proteins are the gene products of the *lhcb4*, *lhcb5*, and *lhcb6* genes and

are called CP29, CP26, CP24, respectively. The *psbS* gene product belongs to the light-harvesting and light energy-regulating protein family but contains hardly any chlorophyll (Funk et al. 1995). The monomeric proteins are less abundant as LHC II but are nevertheless part of the PS II assembly in the membrane.

The structure of a defined PS II assembly – a PS II-LHC II complex of spinach – has been determined to 24 Å by three-dimensional electron microscopy (Nield et al. 2000a). The findings of this study and many others (recent reviews are: Jansson 1994; Hankamer et al. 1997; Barber and Kühlbrandt 1999; Barber et al. 1999) strongly suggest that the PS II-LHC II complex consists of a dimeric PS II core, two copies of the CAB proteins CP29 and CP26, respectively, and two trimeric LHC II. Other CAB proteins like CP24 or PsbS are more loosely associated to the complex. CP24 probably connects a third trimeric LHC II to the core complex, and may bridge two complexes in a side-by-side manner (Boekema et al. 1999a; Yakushevskaya et al. 2001). PsbS was never found in structurally characterized isolates and might form only loose associations with the core complex.

Structural studies on the PS II-LHC II complexes have been focused on spinach (Boekema et al. 1995, Hankamer et al. 1997, Nield et al. 2000a). Amongst other plant species, a complex from *Arabidopsis thaliana*, an angiosperm, and from the green algae *Chlamydomonas Reinhardtii* have been investigated by Yakushevskaya et al. (2001) and Nield et al. (2000a), respectively. These complexes show similar features in electron microscopy analyses when compared to the spinach PS II-LHC II complex, suggesting a similar composition and assembly of the proteins. However, other plant species have not yet been investigated. Liverworts are members of one of the most distant land plant lines relative to the line of angiosperms, and recent studies even indicated that liverworts had split from all other lines first (Bhattacharaya and Medlin 1998; Qiu et al. 1998; Pruchner et al. 2002), which means that the photosynthetic apparatus developed 400 million years in parallel. Thus, some characteristics could be different. Indeed, some light regulation properties of the liverwort *Marchantia polymorpha* are distinct. For example, phosphorylation of the D1 protein, which should protect the plant against a net protein loss during light stress, does not take place in *M. polymorpha* (Schmid et al. 1995; Rintamäki et al. 1995). The liverwort responds to an excess of light by severe photoinhibition and slow recovery, and it accumulates carotenoids in high quantities (Schäfer et

al. 1994). Carotenoids are mainly bound to the CAB proteins, which, interestingly, revealed more basic isoelectric points than those of seed plants (Kilian et al. 1998). CP29 lacks a phosphorylation site (Kilian et al. 1998), which is supposed to be involved in light protection (Bergantino et al. 1995). Furthermore, a strong binding of CP29, CP26, and CP24 to the core complex was observed (Harrer et al. 1998).

This contribution deals with the elucidation of the CAB protein associations with the PS II core complex by Electron microscopy. A characterization of PS II-LHC II complexes from *M. polymorpha* by two- and three-dimensional transmission electron microscopy is presented.

Materials and methods

Culture of Marchantia polymorpha

A starter culture of sterile *M. polymorpha* thallus was kindly provided by E. Beck, institute of plant physiology, university of Bayreuth, Germany. Plants were grown on sterile Gamborg medium (Gamborg's B-5 basal salt mixture, Sigma-Aldrich, Irvine, UK) at a pH of 5.5 at light conditions of ca 70 $\mu\text{mol m}^{-2} \text{s}^{-1}$ for 8 h and 16 h dark, using the growth vessel system by Osmotek (Israel). After 8 weeks in culture, the thalli were harvested at a fresh weight of 3.5 g cm^{-2} culture area. The thalli had a Chl concentration of 0.22 g/g fresh weight and a Chl *a/b* ratio of 2.7.

Isolation of thylakoid membranes

The preparation of thylakoid membranes followed the procedure by Eshaghi et al. (1999): liverwort thallus (500 g) was ground in a solution containing 50 mM HEPES-NaOH pH 7.5, 300 mM sucrose, 5 mM MgCl_2 , 2.5 mM benzamidine, and 1 mM ϵ -amino caproic acid using a Waring blender, and filtered. The filtrate was centrifuged at $1000 \times g$ for 3 min and the pellet was washed once in the same buffer. The washed pellet was suspended in 5 mM MgCl_2 and diluted 1:1 in a solution containing 50 mM MES pH 6.0, 400 mM sucrose, 15 mM NaCl, and 5 mM MgCl_2 . After 10 min centrifugation at $3000 \times g$, the pellet was washed once in a solution containing 25 mM MES pH 6.0, 10 mM NaCl, and 5 mM MgCl_2 . The thylakoid membranes were suspended and stored in a solution containing 25 mM MES pH 6.0, 10 mM NaCl, 5 mM MgCl_2 , and 2 M glycine betaine at a chlorophyll concentration of

2.5 mg ml⁻¹. The membranes were shock-frozen and kept at -80 °C for storage.

Glycerol density centrifugation

Solubilization of the membranes and centrifugation in a glycerol density gradient was performed as described by Harrer et al. (1998) with some modifications. Ultracentrifugation tubes of 1.3 ml volume for a TLS-55 rotor (Beckman, Palo Alto, California) were used. For preparation of the gradient, a solution containing 10 mM Mes pH 6.6, 10 mM NaCl, 5 mM CaCl₂, 0.03% β -dodecyl maltoside (DDM), and 25% glycerol was carefully underlain with the same solution but containing 50% glycerol. The thylakoid membranes (2.5 mg ml⁻¹) were mixed with an equal volume of 2% DDM and, after removing unsolubilized material by centrifugation, applied to the gradient. After 4 h centrifugation at 55 000 rpm in an Optima TLX Ultracentrifuge (Beckman, Palo Alto, California), the green bands were harvested with a syringe. They were shock-frozen and kept at -80 °C for storage.

Electron microscopy

The PS II-LHC II preparation was diluted 1:10 with a solution containing 50 mM EDTA and 0.03% DDM. A small amount of tobacco mosaic virus was added for calibration. An aliquot of 5 μ l of the mixture was applied to a 600 mesh Ni grid coated with a freshly prepared 10 nm layer of carbon. The staining procedure followed the method developed by J. Stoops (Stoops et al. 1992). The grid was washed twice on a drop of water and once on a drop of 2% ammonium molybdate pH 6.5, then transferred to another drop of stain. After 30 s incubation, the liquid was incompletely removed with a filter paper (Whatman 4) touching vertically the edge of the grid for less than a second. Finally, the grid was rapidly dried under a stream of air. Transmission electron microscopy was performed with a Philips Tecnai F20 electron microscope at 120 kV at a calibrated magnification of 51 500 \times . For reconstruction of the particle volume by the Random Conical Tilt technique (Radermacher et al. 1986), a first image was recorded at 55–60° tilt and subsequently a second image of the identical specimen area was recorded without tilt.

Image analysis

Three-dimensional analysis was performed using the Random Conical Tilt method developed by Radermacher et al. (1986). First, 13 pairs of micrographs (from tilted and untilted specimen) were digitized with a 7 μ m pixel size on a Zeiss SCAI scanner. The image size was reduced by averaging 3 \times 3, which results in a pixel size of 21 μ m corresponding to 0.4 nm on the scale of the specimen. A number of 6542 particle projections were interactively selected (each particle was recorded in the 60° and the 0° view, so that in total 13 084 projections, which are 6542 pairs of particles, were achieved). The contrast transfer function was corrected both for 0° images and tilted images (Radermacher et al. 2001). The 0° particle images were rotationally and translationally aligned using the SPIDER image processing software (Frank et al. 1996, Version 4.2 with modifications). A typical top view and a side view projection were arbitrarily selected as references for a multireference alignment procedure based on the correlation of radon transforms of the images. The classification of the images was performed using a neural network algorithm (Marabini and Carazo 1994) as implemented in XMIPP (Marabini et al. 1996) with a field of 9 \times 9 or 7 \times 7 nodes. Between three and five nodes showing significant differences were selected from the map and used as references in subsequent multi reference alignments. Average images were calculated from the classes. If necessary, the procedures were repeated until the self-organizing map showed no significant variation inside the classes. The resolution was determined by Fourier ring correlation (van Heel 1987) and comparison to 5 \times noise. For three-dimensional reconstruction, the rotation angle of each projection of a non-tilted particle was transferred to the corresponding projection of the tilted particle. Each projection now had the information of its rotational angle and its orientation in space (which is the tilt angle). Using the radon transforms of the projections, reconstructions of each class were calculated. Refinement of the volumes was achieved by aligning the Radon transforms of the individual tilt images to the Radon transforms of the initial volumes (Radermacher et al. 1994).

Other methods

Chlorophyll concentration was determined with *N,N*-dimethyl formamide as solvent by the method of Porra et al. (1989). Room temperature absorption

spectra were recorded with a Lambda Bio 40 Perkin Elmer UV/Vis Spectrometer. For SDS-polyacrylamide gel electrophoresis (SDS-PAGE), 6 M urea was included into the gels, and the gels were stained with Coomassie-blue.

Results

Isolation of PS II-LHC II complexes

A typical preparation of PS II-LHC II complexes of *M. polymorpha* is shown in Figure 1. After solubilization of thylakoid membranes, three green bands separ-

ated on a glycerol density gradient (Figure 1A). Band 1 consists of LHC II as concluded from its chlorophyll *a/b* ratio of 1.4–1.6, its absorption spectrum (not shown), and its pattern on a coomassie stained SDS-polyacrylamide gel (Figure 1C). Band 2 contains PS I and ATP synthase proteins as shown by the band pattern on the gel (Figure 1C). Band 3 shows a typical absorption spectrum of a fraction containing PS II-LHC II complexes (Eshaghi et al. 1999; Harrer et al. 1998; Hankamer et al. 1997, Figure 1B). The chlorophyll *a/b* ratio of 2.9–3.1 and the bands on the coomassie-stained gel indicate the presence of both PS II core proteins and CAB proteins. Among the CAB proteins, the presence of CP29, CP26, CP24 and

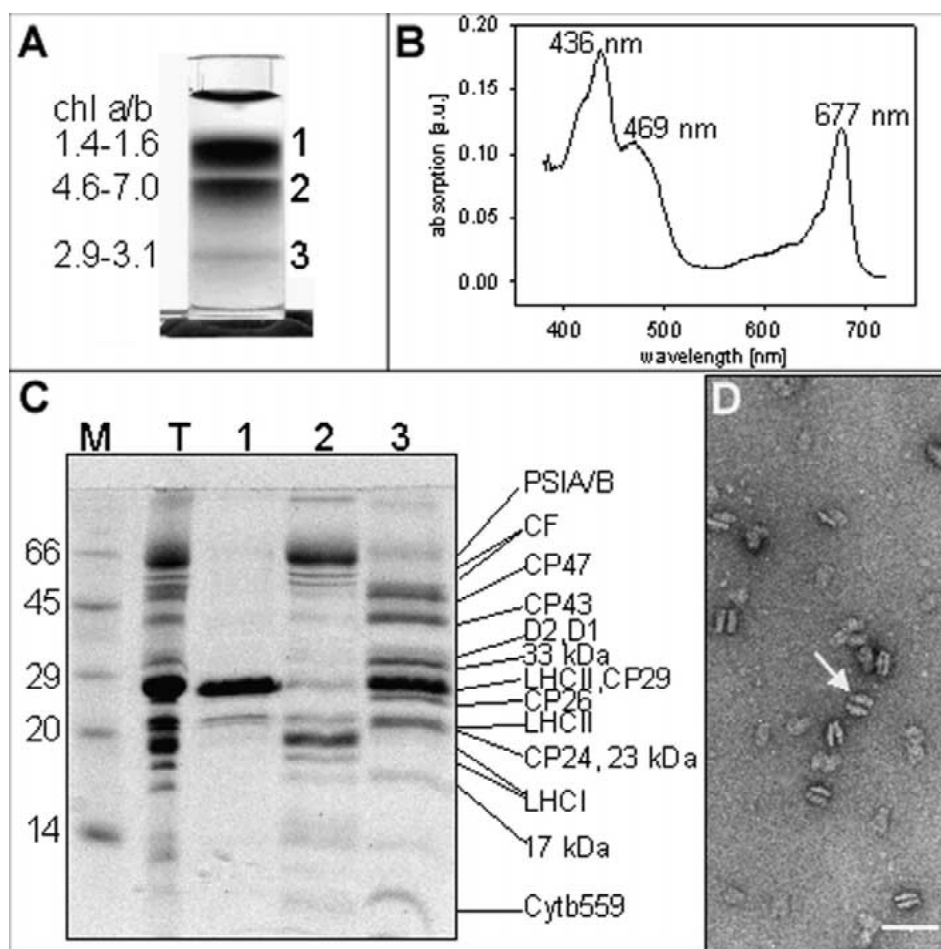


Figure 1. Purification of PS II-LHC II complexes from *M. polymorpha*. (A) Glycerol density gradient of the bands and their chlorophyll *a/b* ratios. (B) Room temperature absorption spectrum of band 3. (C) Coomassie-stained gel of the gradient bands 1–3 (M = marker proteins; T = thylakoid membranes). Assignment of the bands to different proteins is shown. PS I A/B, the A and B protein of PS I; CF, coupling factor (α and β subunits of ATP synthase); 33, 23, and 17 kDa, the extrinsic proteins; LHC I, light-harvesting complex of PS I. (D) Transmission electron microscopy of band 3. The specimen was stained with uranyl acetate. bar = 50 nm.

LHC II was confirmed by their apparent molecular mass in SDS-PAGE and by immunoblotting (data not shown). About 10% of the invested chlorophyll was recovered in this band.

Transmission electron microscopy of the complexes

Initial electron microscopy studies indicated that most of the PS II–LHC II complexes from *M. polymorpha* form assemblies of two particles in contact with each other through their flat surfaces (Figure 1D, arrow). Unfortunately, this structure proved to be unsuitable for three-dimensional image analysis because many of these particle pairs have the two surfaces shifted or rotated relative to each other, or even partly disconnected, making the preparation very inhomogeneous. To overcome this problem, it was decided to disconnect the two halves completely, and then to investigate the particles independently. Because it was assumed that the particle association was caused mainly by Mg^{2+} ions, EDTA was added to the preparation (B. Hankamer, personal communication), which indeed resulted in separation of the two particles (see Figure 2). Moreover, the use of ammonium molybdate pH 6.5 as a stain instead of uranyl acetate reduced the number of particle pairs. Figure 2A shows a typical micrograph of a sample treated with EDTA and stained with ammonium molybdate pH 6.5. Closer inspection of this and many other micrographs by eye led to the conclusion that the preparation was now well suited for three-dimensional analysis, not only because the double particles are reduced to almost zero, but also because the single particles appear homogenous with respect to their size and integrity, and small and broken particles are scarce. Side and top views of the particles are easily distinguished. The side views (marked with an 's') appear as rod-like structures of high contrast and their relation to the top views is nicely seen on the micrograph of the tilted specimen (Figure 2B). Larger structures than those of single particles (asterisks) probably consist of two particles arranged side-by-side. These structures were not included in further analyses because of their obvious high variability.

Two- and three-dimensional image analysis

A typical top view and a side view projection, respectively, were chosen as first references for the two-dimensional alignment of the particles. Both initial classes (the top and the side view) were subjected independently to further classification procedures

based on pattern recognition using neural network algorithms (Marabini and Carazo 1994; see also Radermacher et al. 2001). The classifications yielded four distinct top-view and five side-view classes, whose respective image averages are shown in Figure 3. The top-view class 1 (t1) contains poorly defined particles and was not used for further analysis. The other top-view classes (t2, t3, and t4) contain rectangular or slightly S-shaped structures with or without an additional mass at the side of the particle. A deeper investigation of t4 yielded three new classes (t4-1, t4-2, and t4-3), one of them bearing two additional masses in a symmetrical arrangement (t4-3). Among the side views, different orientations of a bulky mass are obvious (s1 and s2), but other classes differ only in the length and in the bending of the particle. Unfortunately, the side views did not show much information along their axis perpendicular to the view plane, and none of the classes could be related unambiguously to any of the top-view classes. Therefore, it has to be assumed that each of the side-view classes comprises a mixture of particles containing no, one, or two extra masses at the side of the complex. Due to this observation, a reconstruction would not be helpful and accordingly, the side views were not included in the three-dimensional analysis.

Class t2 (854 particles) and, in order to represent all particles with one additional mass at the side of the particle, classes t3, t4-1, and t4-2 (in total 1684 particles aligned and added up) were chosen for three-dimensional reconstruction. Figure 4 shows the rendered surface representations at a resolution of 40 Å. Comparing these surfaces with other structures of PS II–LHC II complexes (Boekema et al. 1995; Hankamer et al. 1997; Nield et al. 2000a, b), luminal and stromal sides could be identified based on the characteristic protrusions of the extrinsic proteins (marked as asterisks). The PS II–LHC II particles from *M. polymorpha* are about 285 Å in length, 144 Å in width and 84 Å in height, while the putative membrane part is about 52 Å thick.

Localization of LHC II

Boekema et al. (1999a, b) suggested that the additional mass at the side of the symmetric PS II–LHC II complex contains trimeric LHC II linked to the core complex by CP24. This was checked for the PS II–LHC II complexes from *M. polymorpha* as follows: The t2 and t3 projections (see Figure 3) were overlaid by a projection of trimeric LHC II structure deter-

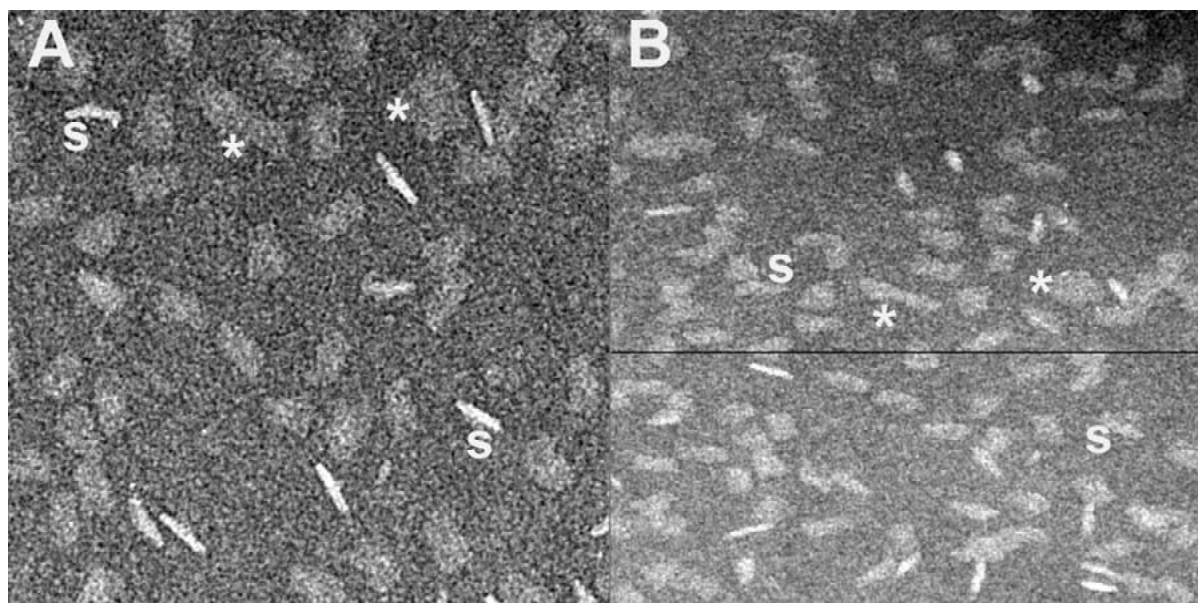


Figure 2. Transmission electron microscopy of band 3, treated with EDTA and stained with ammonium molybdate. (A) The 0° image is shown, and (B) the same area, but tilted by 60° is shown (the horizontal line marks the tilt axis). Side views are indicated by 's'. Asterisks mark particles composed by two side-by-side complexes. bar = 50 nm.

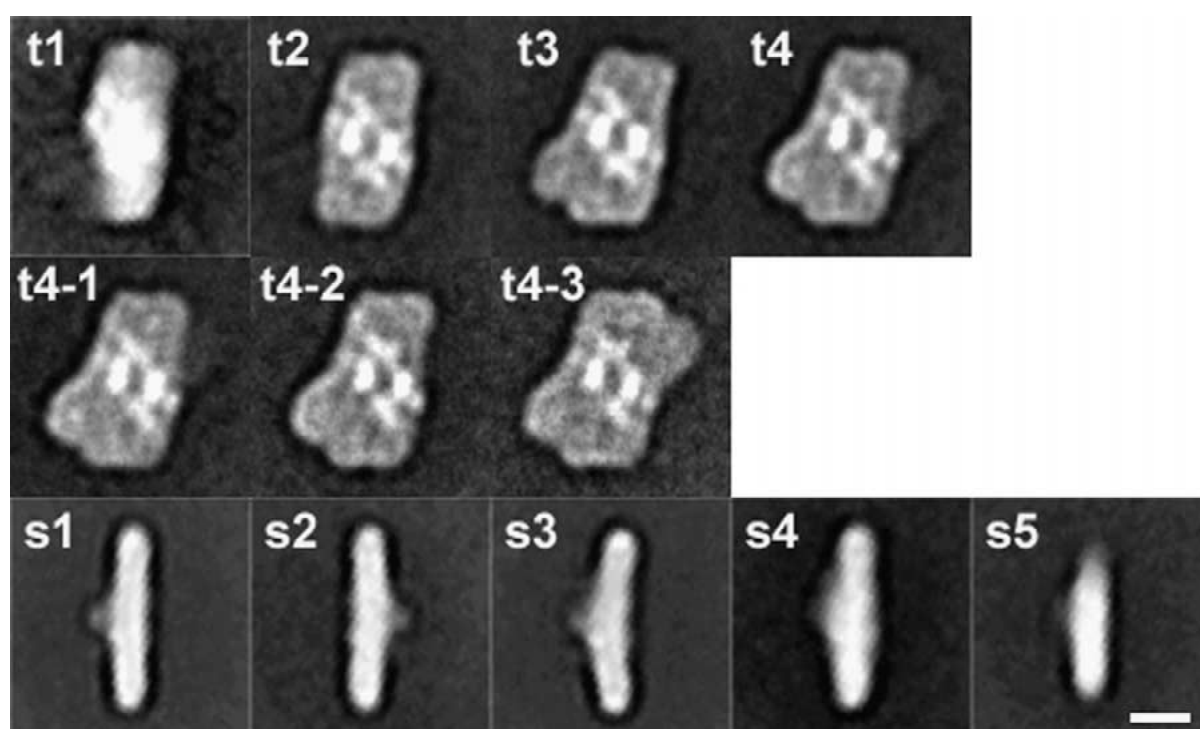


Figure 3. Classification of the top and the side views. Top row: the 2-dimensional averages of the respective top view classes were calculated from 492 (t1), 854 (t2), 862 (t3), and 990 (t4) particles. Middle row: further classification of t4 yielded classes of 175 (t4-1), 272 (t4-2), and 550 particles (t4-3), whose respective averages are shown. Bottom row: the averages of the side views contain 794 (s1), 414 (s2), 614 (s3), 753 (s4), and 358 images (s5), respectively. bar = 100 Å.

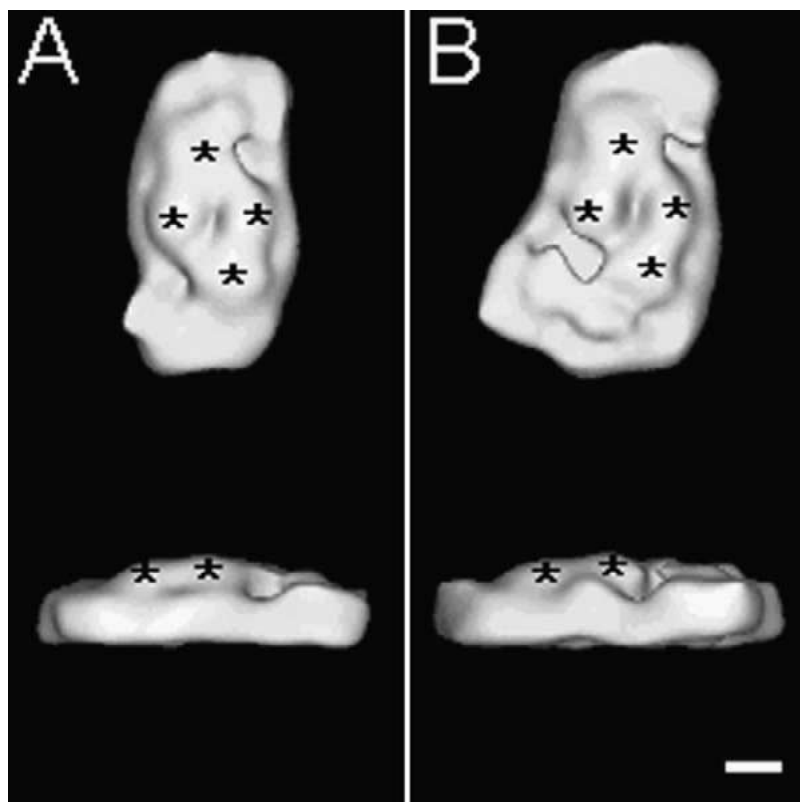


Figure 4. Rendered surface representations of the particles calculated from 854 projections (A) and from 1684 projections (B). The view from the luminal side is shown in the top row, while the side views are presented in the bottom row. Asterisks mark the extrinsic proteins on the luminal side of the complex. bar = 50 Å.

ined by electron crystallography of two-dimensional crystals stained with uranyl acetate (Kühlbrandt et al. 1983). The usage of *stained* LHC II template is important since for the first time, a comparison of PS II–LHC II structures and LHC II recorded under the same conditions has been performed. Figure 5 shows the t2 and t3 projections, whereby lighter areas represent regions of high, darker areas regions of low contrast. The insert represents the map of trimeric LHC II at the same resolution (25 Å). This map served as a template for drawing the outline of the LHC II trimer, which was placed onto one of the putative LHC II sites of the t2 particle (left). Another LHC II-trimer sketch was fitted onto the additional density in the t3 projection (right). Unfortunately, this overlay did not allow a precise localization of the CAB proteins within the PS II–LHC II map due to the low resolution. However, the dimensions of the putative LHC II sites match with those of the LHC II map. Furthermore, a distinct density in the extra mass of the t3 projection (arrow)

indicates an additional CAB protein, which links the LHC II trimer to the core complex.

Discussion

Purification

For the first time, PS II–LHC II complexes have been isolated from *M. polymorpha* plants. A modified purification procedure by Eshaghi et al. (1999) was used, which gave the best results. This method does not involve the preparation of PS II-enriched membranes as an intermediate step, and a short preparation time is achieved (6–7 h from plants to purified complexes), while the treatment with detergents is reduced to a minimum (i.e., no treatment with Triton-X 100). For separation of PS II from PS I and other (smaller) membrane complexes under mild conditions, centrifugation in a glycerol density gradient (Harrer et al. 1998) gave better results than that in a sucrose gradient (Dainese

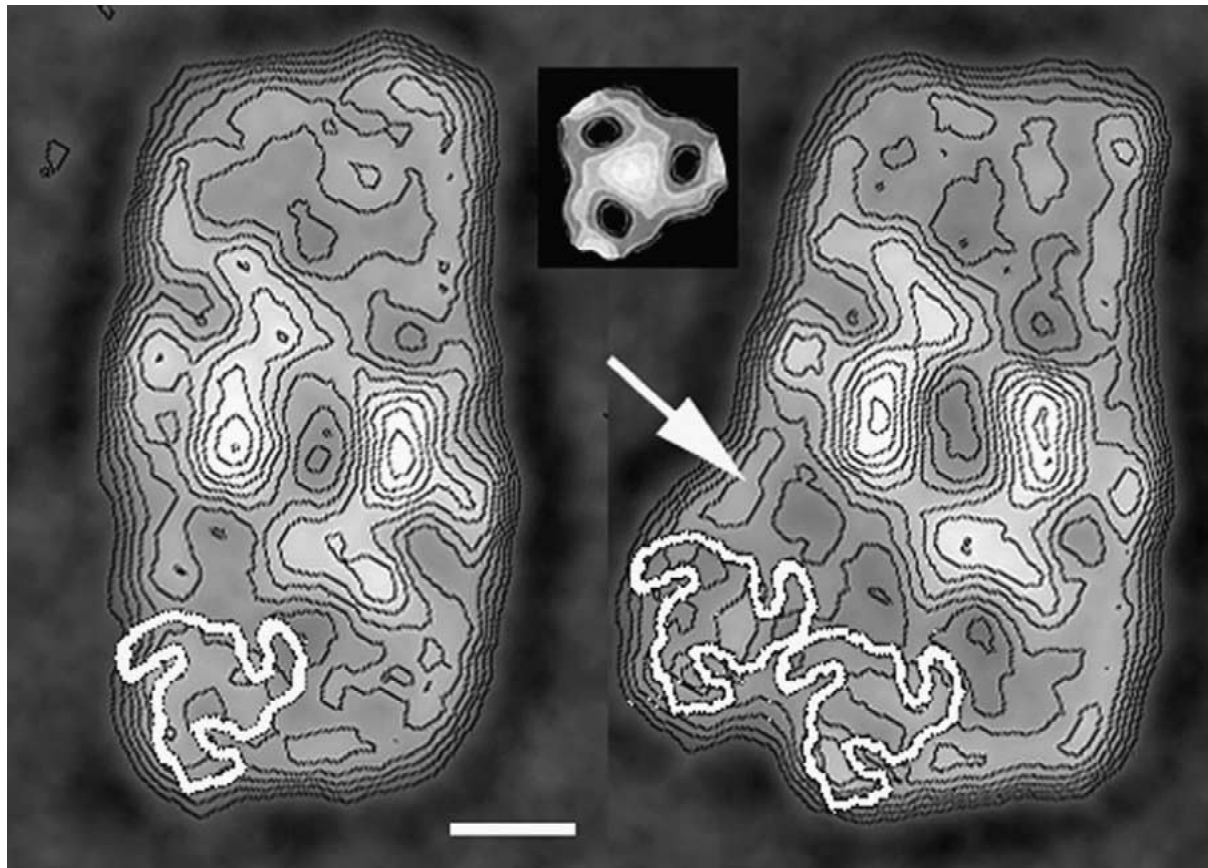


Figure 5. Overlay of the PS II-LHC II class average projections without (left) and with an additional mass at the side (right) with an LHC II projection map (insert) obtained from two-dimensional crystals. The outline of the LHC II map (white) is placed with best fit onto putative LHC II sites of the PS II-LHC II particle. The arrow indicates a protein density, which probably connects the LHC II trimer with the core. bar = 50 Å.

and Bassi 1991; Boekema et al. 1995; Hankamer et al. 1997). However, the relative content of LHC II in the isolates from *M. polymorpha* plants was somewhat lower than that from the formerly used cell-culture system (Harrer et al. 1998), which is indicated by a slightly higher average chlorophyll *a/b* ratio (2.9 compared to 2.7 for the cell culture system).

Structural characterization of PS II-LHC II complexes and localization of LHC II

The particles formed sandwich-like structures when stained with uranyl acetate and investigated by transmission electron microscopy, which is typical for PS II-LHC II complexes isolated by means of a density gradient (Boekema et al. 1995, Hankamer et al. 1997). To divide these sandwiches into two independent halves, a combination of EDTA treatment and

ammonium molybdate stain was successfully applied. Surprisingly, many of the particles, much more as in uranyl acetate stain, are now side views. This can be explained by an increased hydrophobic interaction of the carbon surface with the membrane moiety of the proteins due to the different stain. Glow discharging, which makes the carbon film hydrophilic, did not enhance the number of top views significantly. Unfortunately, the side views carry only very little structural information in the membrane direction, and they could not be classified by their content of CAB proteins. If it is desired to use also the side views for structural studies, the total number of particle images has to be much larger, i.e., a couple of thousand projections more in each class.

The structure of the PS II-LHC II complexes from *M. polymorpha* is remarkably similar to that of PS II-LHC II complexes from other plant species (Boekema

et al. 1999a, b; Nield et al. 2000a, b). The dimensions are equal to those of the complex from spinach (Boekema et al. 1995), from *C. Reinhardtii* (Nield et al. 2000b), and from *A. thaliana* (Yakushevskaya et al. 2001). The extrinsic proteins exhibit a clear rectangular arrangement within the particle (Figure 4), and about 25% of the particles have a rectangular or slightly S-shaped form (class t2), which is the most investigated form of PS II–LHC II particles. Boekema et al. (1999b) named this form the C₂S₂ type (a dimer of the core complex has attached two strongly bound LHC II). Interestingly, 50% of the particles from *M. polymorpha* carry an additional mass at the side. This structure resembles the spinach C₂S₂M type (M stands for medium strongly bound LHC II), which in spinach accounts for only a minor partition of particles (Boekema et al. 1999a), but for much more, 27%, in a preparation from *A. thaliana* (Yakushevskaya et al. 2001). Because of its high abundance in *M. polymorpha*, the C₂S₂M type could serve excellently as a tool for a precise localization of the CAB proteins within the PS II–LHC II complex. Unfortunately, the herein achieved resolution of 25 Å in projection and 40 Å for the reconstructed particle was not enough for this purpose. However, an overlay of the projections with a map of stained LHC II trimer strongly suggested that the tips of the symmetric t2 particle consist of trimeric LHC II, and that the extra mass of the t3 particle contains trimeric LHC II and an additional protein, a putative CAB protein. These results are perfectly in line with the described supramolecular topology of CAB proteins within the PS II–LHC II complex from spinach (Boekema et al. 1999a, b).

In *M. polymorpha*, about 8% of the particles carry two additional masses arranged symmetrically around the PS II core. According to previous considerations, both masses should consist of a trimeric LHC II and a monomeric CAB protein. Also other ('loose') positions for LHC II at the PS II complex have been found for spinach complexes (Boekema et al. 1999b). In this preparation, there is no sign for a further LHC II position, and in the *A. thaliana* preparation it was neither (Yakushevskaya et al. 2001). It is possible that such associations went lost for *M. polymorpha* during the isolation process. Therefore, solubilized PS II membranes without prolonged purification were also investigated (not shown) but other LHC II positions than the reported ones were not observed. Possibly, these special PS II–LHC II associations are extremely seldom.

In conclusion, PS II–LHC II complexes from very different plant species do assemble in the same way. However, the binding of LHC II and other CAB proteins to the core complex seems to be differently strong, and strongest for the liverwort complexes. This is exemplified by the dominance of the C₂S₂M complex in the liverwort isolates.

Acknowledgements

This work was supported by a DFG postdoctoral grant HA 2958. The author thanks W. Kühlbrandt for providing the projection map of negatively stained LHC II at the required resolution. M. Radermacher and T. Ruiz are gratefully acknowledged for advice on the techniques of electron microscopy and image processing. Thanks to J. Nield for helpful discussions.

References

- Barber J and Kühlbrandt W (1999) Photosystem II. *Curr Opin Struct Biol* 9: 469–475
- Barber J, Nield J, Morris EP and Hankamer B (1999) Subunit positioning in Photosystem II revisited. *Trends Biochem Sci* 24: 43–45
- Bassi R, Pineau B, Dainese P and Marquardt J (1993) Carotenoid-binding proteins of Photosystem II. *Eur J Biochem* 212: 297–303
- Bergantino E, Dainese P, Cerovic Z, Sechi S and Bassi R (1995) A post-translational modification of the Photosystem II subunit CP29 protects maize from cold stress. *J Biol Chem* 270: 8474–8481
- Bhattacharaya D and Medlin L (1998) Algal phylogeny and the origin of land plants. *Plant Physiol* 116: 9–15
- Boekema EJ, Hankamer B, Bald D, Kruip J, Nield J, Boonstra AF, Barber J and Rögner M (1995) Supramolecular structure of the photosystem II complex from green plants and cyanobacteria. *Proc Nat Acad Sci USA* 92: 175–179
- Boekema EJ, van Roon H, Calkoen F, Bassi R and Dekker JP (1999a) Multiple types of association of Photosystem II and its light-harvesting antenna in partially solubilized Photosystem II membranes. *Biochemistry* 38: 2233–2239
- Boekema EJ, van Roon H, van Breemen JFL and Dekker JP (1999b) Supramolecular organization of Photosystem II and its light-harvesting antenna in partially solubilized Photosystem II membranes. *Eur J Biochem* 266: 444–452
- Dainese P and Bassi R (1991) Subunit stoichiometry of the chloroplast Photosystem II antenna system and aggregation state of the component chlorophyll *a/b* binding proteins. *J Biol Chem* 266: 8136–8142
- Eshaghi S, Andersson B and Barber J (1999) Isolation of a highly active PS II–LHC II supercomplex from thylakoid membranes by a direct method. *FEBS Lett* 446: 23–26
- Frank J, Radermacher M, Penczek P, Zhu J, Li Y, Ladjadj M and Leith A (1996) SPIDER and WEB: processing and visualisation of images in 3D electron microscopy and related fields. *J Struct Biol* 116: 190–199

- Funk C, Schröder WP, Napiwotzki A, Tjus SE, Renger G and Andersson B (1995) The PS II-S protein of higher plants: a new type of pigment-binding protein. *Biochemistry* 34: 11133–11141
- Hankamer B, Barber J and Boekema EJ (1997) Structure and membrane organisation of Photosystem II in green plants. *Annu Rev Plant Physiol Plant Mol Biol* 48: 641–671
- Harrer R, Bassi R, Testi MG and Schäfer C (1998) Nearest-neighbor analysis of a Photosystem II complex from *Marchantia polymorpha* L. (liverwort), Which contains reaction center and antenna proteins. *Eur J Biochem* 255: 196–205
- Jansson S (1994) The light-harvesting chlorophyll *a/b*-binding proteins. *Biochim Biophys Acta* 1184: 1–19
- Jansson S (1999) A guide to the Lhc genes and their relatives in *Arabidopsis*. *Trends Plant Sci* 4: 236–240
- Kilian R, Bassi R, Testi MG and Schäfer C (1998) Identification and characterisation of Photosystem II chlorophyll *a/b* binding proteins in *Marchantia polymorpha* L. *Planta* 204: 260–267
- Kühlbrandt W, Thaler T and Wehrli E (1983) The structure of membrane crystals of the light-harvesting chlorophyll *a/b* protein complex. *J Cell Biol* 96: 1414–1424
- Kühlbrandt W, Wang DN and Fujiyoshi Y (1994) Atomic model of plant light-harvesting complex by electron crystallography. *Nature* 350: 130–135
- Marabini R and Carazo JM (1994) Pattern recognition and classification of images of biological macromolecules using artificial neural networks. *Biophys J* 66: 1804–1814
- Marabini R, Masegosa IM, Sanmartín MC, Marco S, Fernández JJ, Delafraga LG, Vaquerizo C and Carazo JM (1996) Xmipp – an image processing package for electron microscopy. *J Struct Biol* 116: 237–240
- Nield J, Orlova EV, Morris EP, Gowen B, Van Heel M and Barber J (2000a) 3D map of the plant Photosystem II supercomplex obtained by cryoelectron microscopy and single particle analysis. *Nat Struct Biol* 7: 44–47
- Nield J, Kruse O, Ruprecht J, da Fonseca P, Büchel C and Barber J (2000b) Three-dimensional structure of *Chlamydomonas reinhardtii* and *Synechococcus elongatus* Photosystem II complexes allows for comparison of their oxygen-evolving complex organisation. *J Biol Chem* 275: 27940–27946
- Paulsen H (1995) Chlorophyll *a/b*-binding proteins. *Photochem Photobiol* 62: 367–382
- Porra RJ, Thompson WA and Kriedemann PE (1989) Determination of accurate extinction coefficients and simultaneous equations for assaying chlorophylls a and b extracted with four different solvents: verification of the concentration of chlorophyll standards by atomic absorption spectroscopy. *Biochim Biophys Acta* 975: 384–394
- Pruchner D, Beckert S, Muhle H and Knoop V (2002) Divergent intron conservation in the mitochondrial nad2 gene: signatures for the three bryophyte classes mosses, liverworts and hornworts and the lycophytes. *J Mol Evol* (in press)
- Qiu YL, Cho Y, Cox JC and Palmer JD (1998) The gain of three mitochondrial introns identifies liverworts as the earliest land plants. *Nature* 409: 618–622
- Radermacher M (1994) Three-dimensional reconstruction from random projections: orientational alignment via Radon transforms. *Ultramicroscopy* 53: 121–136.
- Radermacher M, Wagenknecht T, Verschoor A and Frank J (1986) A new three-dimensional reconstruction scheme applied to the 50S ribosomal subunit of *E. Coli*. *J Microscopy* 141: Rp1–Rp2
- Radermacher M, Ruiz T, Wiczorek H and Gruber G (2001) The structure of the V-1-ATPase determined by three-dimensional electron microscopy of single particles. *J Struct Biol* 135: 26–37
- Rintamäki E, Salo R, Lehtonen E and Aro E-M (1995) Rapid turnover of the D1 reaction-center protein of Photosystem II as a protective mechanism against photoinhibition in a moss, *Ceratodon purpureus* (Hedw.) Brid. *Planta* 194: 520–529
- Schäfer C, Schmid V and Ross M (1994) Alterations of the chlorophyll-protein pattern in chronically photoinhibited cells. *Planta* 192: 473–479
- Schmid V, Peter S and Schäfer C (1995) Prolonged high-light treatment of plant cells results in changes of the amount, the localization, and the electrophoretic behavior of several thylakoid membrane proteins. *Photosynth Res* 44: 287–295
- Stoops JK, Kolodziej SJ, Schroeter JP, Bretaudiere JP and Wakil SJ (1992) Structure-function relationships of the yeast fatty acid synthase: negative-stain, cryo-electron microscopy, and image analysis studies of the end views of the structure. *Proc Natl Acad Sci USA* 89: 6585–6589
- Van Heel M (1987) Angular reconstitution: a posteriori assignment of projection directions for 3 D reconstruction. *Ultramicroscopy* 21: 111–123
- Yakushevskaya AE, Jensen PE, Keegstra W, van Roon H, Scheller HV, Boekema EJ and Dekker JP (2001) Supermolecular organisation of Photosystem II and its associated light-harvesting antenna in *Arabidopsis thaliana*. *Eur J Biochem* 268: 6020–6028
- Yamamoto HY and Bassi R (1996) Carotenoids: localisation and function. In Ort DR and Yokum CF (eds) *Oxygenic Photosynthesis: the Light Reactions*, pp 539–563. Kluwer Academic Publishers, Dordrecht, The Netherlands